Effect of Organic SAMs on the Evolution of Strength of Silicon Nanostructures

Scott Grutzik[1], Brian Bush[3], Frank DelRio[3], Richard Gates[3], Melissa A. Hines[2], Alan Zehnder[1]

[1]Field of Theoretical and Applied Mechanics,
Cornell University, Ithaca, NY 14853
[2]Department of Chemistry and Chemical Biology,
Cornell University, Ithaca, NY 14853
[3]Nanomechanical Properties Group, Material Measurement Laboratory,
National Institute of Standards and Technology, Gaithersburg, MD 20899

Abstract

The ability to accurately predict the strength of nanoscale, single crystal structures is of interest in micro- and nanoelectromechanical systems (MEMS and NEMS) design. Because of the small length scales involved failure does not always follow the same trends as at larger sizes. Due to low defect density and high surface to volume ratio, failure is primarily dependent on surface features. Previous work has shown that oxidation of the surface of silicon nanostructures correlates to decreased strength and that methyl surface monolayers can be used to slow oxidation and maintain initial strength. We extend these results to use longer chain self-assembled monolayers (SAMs) prepared in a variety of ways. Although only initial results are included here, aging will be carried out over a much longer time period than in previous studies. Fracture tests were performed using an atomic force microscope (AFM) following a method previously demonstrated by Alan, *et al.*

Introduction

Micro- and nanoelectromechanical systems (MEMS and NEMS) play an increasing role in many fields such as telecommunications, defense, microelectronics, and biomedical devices. These systems can be subjected to sustained loads, oscillating loads, dynamic shock loading, or a combination of all three. For example, if a device is desired to operate in the megahertz frequency range for at least five years it must withstand 10^{14} to 10^{15} repeated loadings. The small size of these devices make accurate predictions and measurements of strength and durability difficult. As a result they may be designed with overly large factors of safety with respect to mechanical failure. More efficient design will require accurate knowledge of the stochastic nature of fracture at these length scales.

For a variety of reasons, it is difficult to extrapolate macroscale material failure behavior down to the length scales required for MEMS and NEMS design. Components of these systems are often small enough that they contain few or no defects other than those introduced during processing. Also, because of their high surface to volume ratio, surface properties tend to play a larger role than volumetric properties. Nonetheless, it is possible to make some general predictions. From a continuum mechanics perspective, a smoother surface should give rise to a stronger structure. Any pit or ledge on the surface will act as a stress concentrator under loading and act as a potential nucleation point for fracture. It is also expected that if the surface can be maintained in a compressive state, strength should increase. The compressive stress would act to hold the faces of any existing cracks together, making it more difficult for cracks to propagate.

Alan, *et al.* have reported results that agree with the first of these expectations. Their results suggest that the surface roughness of nanoscale Si beams strongly affects their strength and that if the surface is smooth enough the strength can be close to the ideal strength derived from atomistic simulations [1]. Alan, *et al.* have also reported results that are somewhat at odds with the second expectation that a compressive surface stress should increase fracture strength. Their data shows a decrease in strength with increasing surface oxidation and that if oxidation is prevented the initially high strength is maintained [2]. What makes this an unexpected result is that silicon dioxide grown on a Si surface grows in a compressive state. From our continuum mechanics reasoning oxidation should lead to an increase in fracture strength, not a decrease as the data suggests. The work presented here is part of an effort

to understand the mechanisms behind how oxidation affects nanoscale strength.

As previously noted, Alan *et al.* showed that oxidation over time and the subsequent decrease in fracture strength can be averted through careful modification of the surface to include a monolayer-thick methyl coating [2]. As an alternate means of suppressing surface oxidation, long chain n-alkylsilane $[CH_3(CH_2)_{n-1}SiCl_3, n \geq 2]$ self-assembled monolayers (SAMs) may be adsorbed onto the surface to produce highly hydrophobic protective coatings. The long chain n-alkylsilane coatings provide improved interfacial mechanical properties that may be of interest to MEMS designers. These properties include lower works of adhesion, small interfacial shear strengths, and increased wear resistance [3, 4]. Although long chain n-alkylsilane SAMs do not covalently bond to every surface bonding site of the Si(111) surface as in the methyl termination [5] , the high hydrophobicity and greater ultimate film thicknesses may provide for comparable levels of long-term oxidative stability while simultaneously improving the aforementioned interfacial mechanical properties.

Sample Fabrication
Accurate measurement of mechanical properties such as stiffness or fracture strength on micro- and nanoscale samples is difficult. The small sizes and forces involved introduce challenges at every step of the process, from sample fabrication to gripping the specimen to measuring small forces and displacements. Several methods have been proposed, including adapting macroscale techniques like three point bending to the nanoscale [6], high precision piezo-controlled loading devices [7], high throughput tests consisting of a chain of nanoscale rings [8], and a test specimen shaped like the Greek letter Θ which allows the crossbar to be easily put in a state of pure tension [9]. Each of these approaches has advantages and disadvantages. The chain of rings method, for example, can produce a lot of data with relatively little effort but requires a complex fabrication process and special testing apparatus.

Here we use a method developed by Alan, *et al.*[1, 2] similar to that of Namazu, *et al.* [6] in which a force is applied at the midpoint of a suspended single crystal beam via an atomic force microscope (AFM). A scanning electron micrograph of such a beam after testing is shown in Figure 1. The test specimens are fabricated from Si (111) wafers using standard micro-machining techniques in the process outlined in Figure 2 [10]. The long axis of the beam is parallel to the $[1\bar{1}0]$ direction.
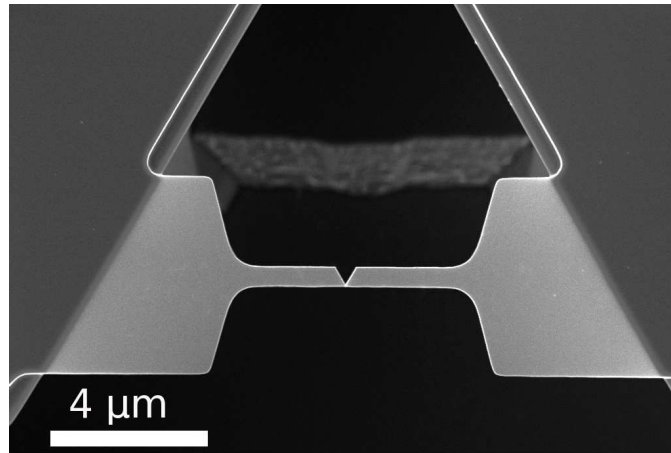

Figure 1: Scanning electron micrograph of a fractured nanobeam. The V shaped notch is not part of the fabricated design but a characteristic of the failure mode.

The "dog bone" shape of the sample ensures that the fracture stress occurs reproducibly in the center of the beam, where the small width leads to highest stress. If the beam were uniform width, there would be stress concentrations at the attachment points which would complicate analysis.

The fabrication process involves using two consecutive steps of photolithography and reactive ion etching. The first lithography and etch step, denoted by (a) in Figure 2, defines the shape of the beam. The depth of this first etch roughly controls the thickness of the beam. After the first etch step, a 100 nm layer of thermal oxide is grown,
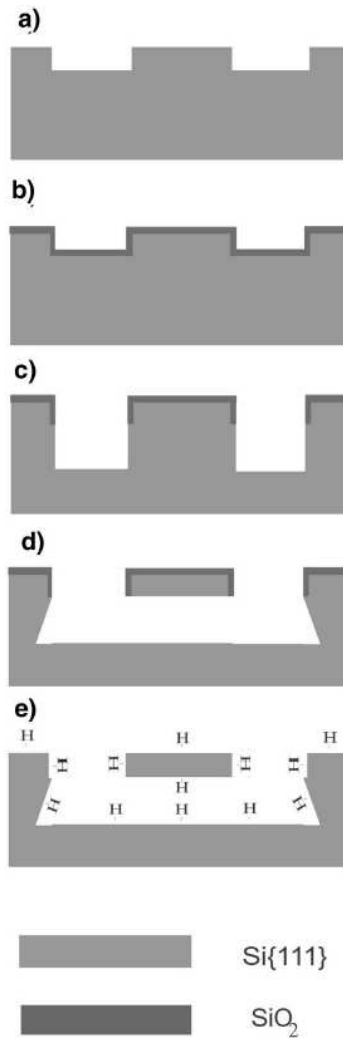
Figure 2: Diagram of Si nanobeam fabrication process

as shown in Figure 2(b). A second round of lithography and etching defines a deep trench on both sides of the beam. After this step, the beam is still connected to the substrate by a pillar of Si.

The beams are released with an anisotropic etchant that rapidly removes all non-{111} exposed Si surfaces, leaving behind an atomically clean, H-terminated surface. To prevent uncontrolled oxidation of the H-terminated surface, the beams are only released just prior to fracture testing. The unreleased beams are first cleaned with a modified RCA clean [11]. The RCA cleaning procedure involves immersing the beams in 5:1:1 solution of H_2O (water), H_2O_2 (hyrdogen peroxide), and NH_4OH (ammonium hydroxide) at 80°F for 10 minutes followed by immersion in a 5:1:1 solution of H_2O, H_2O_2, and HCl (hydrochloric acid) at 80°F for 10 minutes. The first solution removes any organic contaminants and the second any metallic contamints. The beams are then anisotropically etched with potassium hydroxide (KOH) and tetramethyl ammonium hydroxide (TMAH). These etchants produce the Si {111} terminated structure in Fig 2(e). This procedure slowly etches the backside of the beam; however, top and sides of the beam are protected by the oxide layer. The oxide layer is then removed with a buffered oxide solution (a 5:1 mixture of NH_4F:HF) and rinsed in ultrapure water. This leaves all surfaces hydrogen terminated.

After the removal of the oxide layer, samples that are to be SAM coated undergo two divergent procedures: First, hydrogen terminated samples are directly immersed in n-aklylsilane solutions. Second, some samples are subjected to reoxidation via an ultraviolet ozone (UV-O_3) treatment for 10 minutes, leading to the growth of a chemical oxide

of with a thickness of 1.3 nm as measured by spectroscopic ellipsometry. The UV-O$_3$ grown chemical oxide results in more complete silanization of the surface producing SAMs that are more robust and densely packed than their non-oxide counterparts [12].

Following the reoxidation step, both chemically oxidized and H-terminated samples are immersed in 2 mM n-alkylsilane solutions of 3:2 hexadecane and carbon tetrachloride in a glovebox with a relative humidity of approximately 8%. Alkylsilanes of $n = 5$ were obtained from Santa Cruz Biotechnology (Santa Cruz, CA) and those of $n = 18$ from Sigma Aldrich (Milwaukee, WI). Chemically oxidized samples are allowed to react for 90 minutes, while the H-terminated surfaces are immersed for 90 minutes and 24 hours. Upon removal from the SAM solution, the samples are rinsed in fresh hexadecane:carbon tetrachloride solvent, isoproponal, and then dried under a stream of dry N$_2$. This results in highly hydrophobic SAM surfaces with water contact angles approaching 98.0 and 107.7 for $n = 5$ and $n = 18$ oxidized surfaces, respectively. Non oxidized samples exhibited slightly lower water contact angles due to the absence of a well-formed oxide layer for covalent siloxane bonding with angles reaching a maximum of 92.9 and 103.3 after 24 hours for $n = 5$ and $n = 18$, respectively.

Fracture Testing Procedure
After fabrication and chemical modification, an AFM is used to apply a force at the center of the beam, as shown in Figure 3. This method has been previously used by Alan, *et al.* The test has two parts. First, the beam is imaged by scanning the AFM cantilever over its surface to obtain its shape. Once the center of the beam is located, the cantilever is brought to this point and pushed straight down until the beam breaks. During the deformation, the displacement applied to the base of the cantilever by the peizo in the AFM head, δ_{piezo}, and the output signal of the photodetector are recorded simultaneously until the beam fractures, as indicated by a sharp discontinuity in photodetector signal. Importantly, both the cantilever and the beam bend during this process. By repeating this deflection test on an effectively rigid area of the wafer surface, the photodetector signal can be calibrated to the cantilever deflection, $\delta_{\mathrm{cantilever}}$. The beam deflection, δ_{beam} is then calculated from $\delta_{\mathrm{beam}} = \delta_{\mathrm{piezo}} - \delta_{\mathrm{cantilever}}$. If the stiffness of the AFM cantilever is known, $\delta_{\mathrm{cantilever}}$ can be converted to the force F applied to the beam. This procedure quantifies the applied force F and beam deflection δ_{beam} at the time of failure.

Before the beam deflection and applied force at failure can be converted to maximum stress at failure, the thickness of the beam must be determined. To do this, we measure the the resonant frequency of the beam by driving it inertially with a swept sine signal. Deflection during this measurement is transduced by optical interferometry. [10]. The in-plane dimensions of the beam can be measured using SEM or the initial AFM scan which was used to locate the beam center. The thickness can then be calculated using the finite element method (FEM). The thickness in the FEM model is adjusted until the calculated resonant frequency agrees with the measured one. The validity of the FEM model can be verified by including higher order resonant frequencies in the thickness determination and by comparing the shape of the FEM generated load-deflection curve prior to failure to the experimental one. In both the physical and finite element beams, the long axis is aligned with the $[1\bar{1}0]$ direction. The material is assumed to be orthotropic with linear elastic modulii $C_{1111} = 166$ GPa, $C_{1212} = 64$ GPa, and $C_{4444} = 79.6$ GPa [13]. All strength testing was done on an Asylum MFP3D AFM (Asylum Research, Santa Barbara, CA). Finite element simulations were peformed using ABAQUS (Dassault Systèmes, Waltham, MD) By applying the force at fracture to this FEM model, the fracture stress can be calculated.

Although only initial strength data is presented here, fracture strength will be measured over a period of 12 to 18 months. Between strength tests the beams are stored in a 100% relative humidity environment at room temperature. This should ensure a constant oxidation rate for the entire aging process.

Preliminary Data
Figure 4 shows a typical force-deflection curve of one of the silicon beams from onset of loading to failure, indicated by termination of the blue line. The structural response of the beam is governed by geometric nonlinearity. As the center of the beam is pushed by the AFM cantilever the ends remain fixed and the entire beam is put in a state of tension. The resulting membrane stress vastly overwhelms the linear bending behavior. Even though linear bending is negligible in the total structural response of the beam, bending is sharply localized near where the load is applied. As a result, a significant portion of the fracture stress does result from bending.

Because silicon fails in a stochastic manner, a number of beams are broken for each type of surface treatment
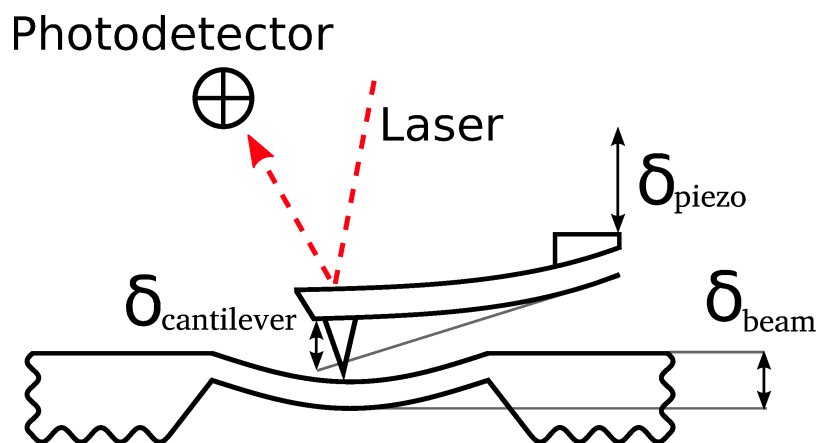
Figure 3: Side view schematic of the AFM based fracture testing process
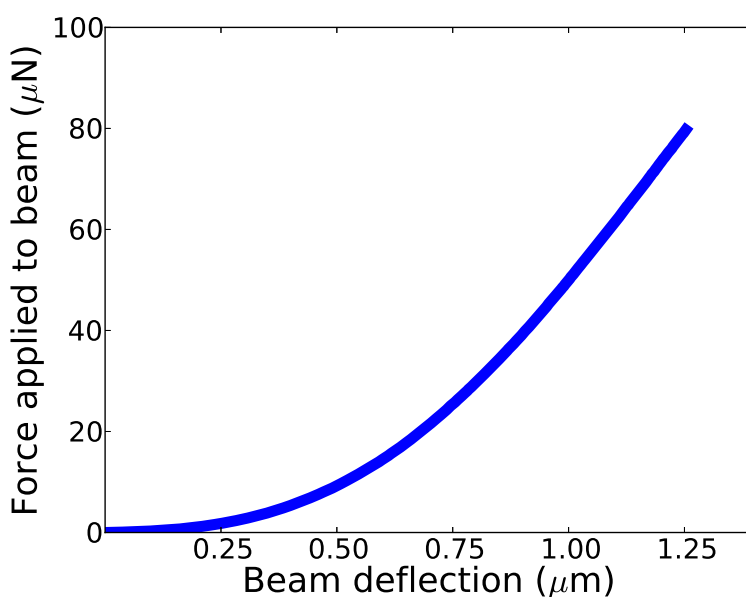

Figure 4: A typical force-deflection curve for a silicon beam from onset of loading to failure

and Weibull strength analysis is performed on each data set. As an example, Figure 5 shows the Weibull fit for the C_{18} sample with a native oxide. The Weibull strength and shape parameters for all eight samples are shown in Table 1.

It should be noted that this data is preliminary for two reasons. First, while we are interested in the evolution of strength for each sample, the strength data here is only the initial strength measured shortly after SAM deposition. Complete, time dependent data is forthcoming. In addition, these fracture stress data were calculated using an estimated, nominal beam thickness. In order to calculate the thickness by measuring resonant frequency as described above the Si chip must be soldered to a piezo which acts as a driving frequency. A low temperature indium solder is used but there is still some risk of damaging the organic SAMs with the elevated temperature. For this reason, final thickness calculations will be made only after all strength measurements are taken. While an error in thickness will affect calculated fracture stresses, because all beams on a chip are assumed to have equal thickness strength data for a given sample will be affected equally. Thickness is only expected to be nominally similar from chip to chip. In light of this, comparisons of strength between samples should not be done at this point. Once final thickness calculations are completed, such comparisons will be possible.
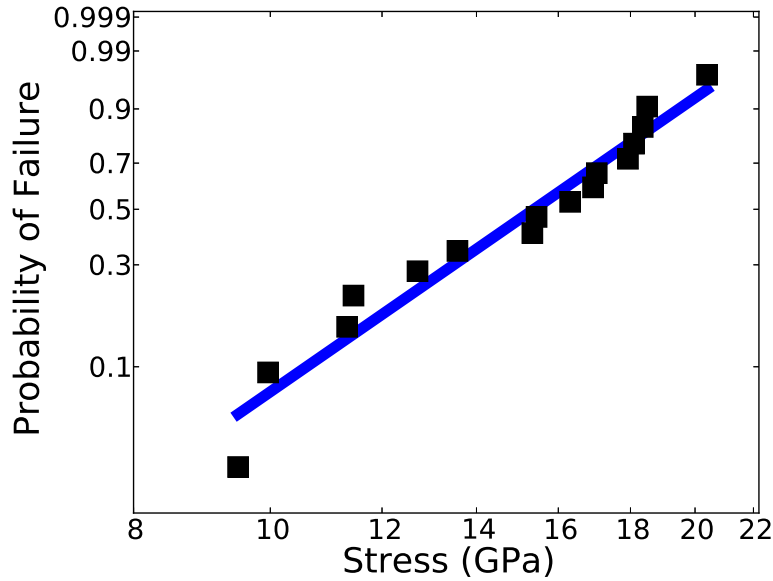
Figure 5: Strength data and Weibull fit for the C_{18} sample with a native oxide

SAM with native oxide			
	H-terminated	C_5	C_{18}
Weibull Strength (GPa)	18.4	17.3	16.5
Shape Parameter	16.9	11.4	5.1

SAM without native oxide					
	H-terminated	C_5 90 min	C_5 24 hr	C_{18} 90 min	C_{18} 24 hr
Weibull Strength (GPa)	14.4	15.6	16.5	11.0	15.6
Shape parameter	11.6	6.0	3.9	10.2	12.3

Table 1: Weibull strength and shape parameters for all samples surface treatments

Summary
We use the method developed by Alan, *et al.* to measure the fracture strength of nanoscale Si beam structures. Previous results have shown that oxidation of the surface of the Si is correlated with a decrease in strength and a methyl monolayer can be utilized to slow oxidation and maintain initial strength [2]. We are working to extend these results to the use of longer chain self-assembled monolayers (SAMs) of length 5 and 18. The SAM coating will result in a highly hydrophobic surface and perhaps other desirable traits such as increased wear resistance. Over the next 12 to 18 months we will be tracking how the strength of each of these sets of beams change. An estimate of the initial strengths are presented here. Because the beam thickness has not yet been measured these should not be taken as final results.

References

[1] T. Alan, M. A. Hines, and A. T. Zehnder. Effect of surface morphology on the fracture strength of silicon nanobeams. *Applied Physics Letters*, 89:091901, 2006.

[2] T. Alan, A. T. Zehnder, D. Sengupta, and M. A. Hines. Methyl monolayers improve the fracture strength and durability of silicon nanobeams. *Applied Physics Letters*, 89:231905, 2006.

[3] B. G. Bush, F. W. DelRio, C. Jaye, and R. F. Cook. Interfacial mechanical properties of n-alkylsilane monolayers on silicon substrates. *J. of Microelectromechanical Systems*, 22(1):34–43, 2013.

[4] U. Srinivasan, J. D. Foster, U. Habib, R. T. Howe, R. Maboudian, D. C. Senft, and M. T. Dugger. Lubrication of polysilicon micromechanisms with self-assembled monolayers. In *Proc. 1998 Solid-State Sensors and Actuators Workshop*, pages 156–161, 1998.

[5] L. J. Webb and N. S. Lewis. Comparison of the electrical properties and chemical stability of crystal silicon (111) surfacse alkylated using grignard reagents or olefins and lewis acid catalysts. *J. Phys. Chem. B*, 107:5404–5412, 2003.

[6] T. Namazu, Y. Isono, and T. Tanaka. Nano-scale bending test of Si beam for MEMS. In *The Thirteenth Annual International Conference on Micro Electro Mechanical Systems*, pages 205–210, 2000.

[7] T. Tsuchiya, O. Tabata, J. Sakata, and Y. Taga. Specimen size effect on tensile strength of surface micromachined polycrystalline silicon thin films. *Journal of Microelectromechanical Systems*, 7:106–113, 1998.

[8] Jr. E. D. Reedy, B. L. Boyce, III J. W. Foulk, Jr. R. V. Field, J. A. Ohlhausen, M. P. de Boer, and S. S. Hazra. Predicting fracture in micron-scale polycrystalline silicon MEMS structures. Technical Report SAND2010-6701, Sandia National Laboratory, 2010.

[9] M. S. Gaither, F. W. DelRio, R. S. Gates, Jr. E. R. Fuller, and R. F. Cook. Strength distribution of single-crystal silicontheta-like specimens. *Scripta Materialia*, 63(4):422–425, 2010.

[10] Y. Wang, J. A. Henry, A. T. Zehnder, and M. A. Hines. Surface chemical control of mechanical energy dissipation in micromachined silicon devices. *Journal of Physical Chemistry B*, 107:14270, 2003.

[11] W. Kern and D. A. Puotinen. Cleaning solutions based on hydrogen peroxide for use in silicon semiconductor technology. *RCA Rev.*, 31:187–206, 1970.

[12] J. B. Brzoska, I. B. Azouz, and F. Rondelez. Silanization of solid substrates: A step toward reproducability. *Langmuir*, 10(11):4367–4373, 1994.

[13] H. J. McSkimin. Measurement of elastic constants at low temperatures by means of ultrasonic wavesdata for silicon and germanium single crystals, and for fused silica. *Journal of Applied Physics*, 24(8):988, 1953.